1 **Quantifying the distribution of swordfish (*Xiphias gladius*) density in the Hawaii-based**
2 **longline fishery**

3 Michelle L. Sculley and Jon Brodziak
4 [a]NOAA NMFS Pacific Islands Fisheries Science Center, 1845 Wasp Blvd, Bldg 176, Honolulu, Hawaii 96818, USA

5 **Abstract**
6 The Hawaii-based longline fishery targeting bigeye tuna and swordfish is the most economically
7 important fishery in Hawaii. An improved understanding of the distribution of swordfish within
8 this fishery and how it changes in response to environmental conditions is critical for predicting
9 potential climate change impacts to the fishery. The multi-species Vector-Autoregressive Spatio-
10 Temporal (VAST) model was used to estimate abundance and density of swordfish within the
11 Hawaii-based longline fishing grounds. Swordfish and bigeye tuna catch per unit effort were
12 used in a spatial dynamics factor analysis to help estimate swordfish density in time periods
13 when the swordfish fishery was closed. Although the model was unable to account fully for the
14 significant changes in fishery regulations in 2000, it provided quantified estimates of swordfish
15 density and distribution and information on how those distributions may change in response to
16 environmental variables. Swordfish density center of gravity was found to correlate with the
17 Southern Oscillation Index (SOI) averaged during the swordfish spawning season (April – July),
18 with densities centered further north and east during positive SOI (cooler sea temperatures) and
19 further south and west during negative SOI (warmer sea temperatures).
20

24 Michelle L. Sculley[a] (corresponding author), michelle.sculley@noaa.gov
25

1. Introduction

Broadbill swordfish (*Xiphias gladius*) inhabit the Pacific Ocean between 50°N and 50°S. They are an economically important species and have supported large-scale longline fishing operations in the Atlantic, Pacific, and Indian Oceans. Adult swordfish are believed to move to foraging grounds along frontal boundaries and coastal boundary currents after spawning, although data on swordfish movements and spatial structure are limited(Bigelow et al., 1999; Dewar et al., 2011; Seki et al., 2002). There are often major challenges studying highly migratory species' stock structure and migratory patterns as these types of investigations are expensive and difficult to implement across the species' possible range. Some electronic tagging of swordfish has been undertaken to better understand both their vertical and horizontal movements (Abecassis et al., 2012; Dewar et al., 2011) and some genetic studies have attempted to identify swordfish stock structure (Lu et al., 2016).However, significant uncertainty remains in our understanding of North Pacific swordfish seasonal movements and density in space.

Fishery-dependent data are often used to help understand swordfish distribution (Ichinokawa and Brodziak, 2010) as fisheries often provide data over a much larger area of the distribution than it would be possible to sample in a fishery-independent survey. These data are not without their own unique challenges. While valuable for assessing the spatio-temporal relationships between abundance and environmental variables, fishery-dependent data have less power for discriminating spatial patterns in encounter rates than fishery-independent data (Pennino et al., 2016). Also, fishery-dependent data can be constrained or biased due to fishing regulations and misreported catches (Pennino et al., 2016). Placing observers on board commercial fishing vessels can reduce some of the drawbacks of fishery-dependent data by ensuring reported catch is more accurate. Additionally, distribution can be correlated with environmental factors such as sea surface temperature, oceanographic fronts, the mixed layer depth, the oxygen minimum zone, and climatological indices which can encompass multiple changes in the environment (Abecassis et al., 2012; Bigelow et al., 1999; Chang et al., 2013; Dewar et al., 2011; Gilman et al., 2007; Howell et al., 2008; Prince and Goodyear, 2006; Seki et al., 2002).

North Pacific swordfish are caught primarily by the Japanese, Taiwanese, and U.S. longline fisheries (Bigelow et al., 1999). The majority of the North Pacific catch comes from the western Pacific associated with the Kuroshio Current (Sakagawa, 1989). However, the shallow-set sector of the Hawaii-based longline fishery targets swordfish. Domestic U.S. longline vessels have been operating in the Hawaii Exclusive Economic Zone since the 1920s, primarily targeting tunas (Boggs and Ito, 1993). Vessels began targeting swordfish in the early 1990s, and the fleet accounted for 40% of the total U.S. swordfish catch in 2012.

Observers were first placed onboard Hawaii-based longline vessels in 1994.There have been several changes to the reporting regulations since its implementation in 1994 (Pacific Islands Regional Office, 2017). These changes have resulted in challenges when standardizing longline catch per unit effort (CPUE) data for the Hawaii-based fishery because it can be difficult to account for changes in catchability due to management regulations (Campbell, 2004) and it can be difficult to include all factors that affect catchability into a standardization (Wilberg et al., 2009). These regulations have included changes in hook type from J-hooks to circle hooks (Pacific Islands Regional Office, 2017), which has been shown to lead to changes to CPUE for billfish on pelagic longlines (Pacheco et al., 2011; Prince et al., 2002). Additionally, the expansion of the Papahanaumokuakea Marine National Monument in 2016 and the periodic closures due to protected species interactions (Pacific Islands Regional Office, 2018) can also

impact catchability because catchability can change seasonally and between areas (Walters, 2003; Ye and Mohammed, 1999).Currently, catch-per-unit effort data are standardized as three different fleets: one deep-set fleet from 1995–present and two shallow-set fleets from 1994–2000 and 2005-present (Sculley et al., 2018b) to account for the changes in operations due to targeting and management regulations. However, incorporating three fleets instead of one into a stock assessment model increases the number of parameters needed to be estimated for the fishery, which could decrease the precision of the model results.

The multi-species Vector-Autoregressive Spatio-Temporal model (VAST) developed by Thorson and Barnett (2017) has the potential to eliminate some of the challenges presented with standardizing the Hawaiian swordfish CPUE data. VAST simultaneously estimates spatio-temporal variation in density for multiple species by applying a delta model to estimate the probability of encounter and catch rate given a positive encounter for a particular location, taxon, and time-step (Thorson and Barnett, 2017). Generally, the fishing area for bigeye tuna is further south than that for swordfish; however, there is considerable overlap. We use the dissimilarities between the expected probability of encounter and catch rate between swordfish and bigeye tuna to account for the differences in gear settings. By doing so, it may be possible to use the entire set of data to produce a CPUE time series including predicted abundance during the closure of the swordfish fishery and fill in the time-period of swordfish relative abundance using only the deep-set data that is currently excluded from the CPUE standardization used in the assessment. Furthermore, a spatial model can help better quantify the distribution of swordfish within the Hawaii-based longline fishing grounds and provide information on how the distribution may be changing over time and in response to environmental conditions. This work will apply the multi-species VAST model to the Hawaii-based longline observer dataset and discuss the distribution and relative density of swordfish around Hawaii, the reliability and challenges of obtaining an annual index of relative abundance for the fishery, and how the distribution of swordfish changes in response to climatological conditions.

2.Methods
2.1 Data

The Hawaii-based longline fleet fishes primarily between the equator and 35°N latitude and 180° W and 125° W longitude. It targets swordfish within and near the Sub-Tropical Convergence Zone north of Hawaii in the winter and late spring (DeMartini et al., 2007).Swordfish are believed to spawn around the Hawaiian Islands from April – July, and small young-of-the-year swordfish are caught in September and October (Demartini et al., 2000).Swordfish catch peaked in 1993, with almost 6,000 mt landed in Hawaii but has since declined to only around 1,000 mt in 2016 (Ito and Childers, 2018).

In the Hawaii longline fishery, swordfish are targeted in the shallow set fishery sector (<15 hooks per float) and as bycatch in the tuna-targeting, deep-set fishery sector (≥15 hooks per float, Ito and Childers, 2018). The number of permitted vessels in the Hawaii-based longline fishery was capped in 1994 to 168 licenses, and the number of vessels targeting swordfish each year decreased from around 100 in the 1990s and has been around 30 since 2000 (Ito and Childers, 2018). Due to interactions with protected sea turtles, the shallow-set swordfish fishery was closed from February 2001 to May 2004 due to interactions with protected sea turtles (Gilman et al., 2007). During this time, many vessels targeting swordfish began targeting tuna. A second closure occurred from March to December 2006 when the Hawaii-based shallow-set longline swordfish fishery reached the annual limit for interactions with loggerhead sea turtles (NMFS, 2017). Shorter closures have occurred periodically since 2006 (Ito and Childers, 2018).

The Pacific Islands Regional Observer Program (PIROP) provides detailed set-by-set data on the Hawaii-based longline fishery including catch in numbers of fish and a variety of operational variables, including: location as latitude and longitude, vessel ID, hooks per float, total number of hooks set, type of bait used, and time longlines were set. The data are collected following the procedures outlined in the PIROP observer manual (Pacific Islands Regional Office, 2017). There have been several changes to the reporting regulations in PIROP since its onset in 1994 (Pacific Islands Regional Office, 2017). Observer coverage varied significantly prior to 2000, with observer coverage between 3.3 and 10.4 % for the entire fishery (NMFS, 2017). Starting in 2001, the observer program had a target of 20% observer coverage on deep-set longline vessels and mandatory 100% observer coverage on shallow-set longline vessels. The data are generally considered high quality since swordfish and bigeye tuna are typically not misidentified by the observers (Walsh, 2000). Observers are placed on board deep-set longline vessels using a randomized statistical survey design that helps ensure the data collected are an unbiased representation of the fishing activities of the deep-set sector.

Data were extracted from the PIROP database on 10 October 2017 for this analysis. Data were filtered so that there were at least three vessels fishing within a 1°x1° square for confidentiality. Data were not spatially aggregated prior to analysis but used on a set-by-set basis because data aggregation has been shown to decrease the performance of spatio-temporal models (Thorson et al., 2017a).There were 686,760 total swordfish and bigeye tuna CPUE data points from almost 350,000 sets.

The environmental variables used in the standardization were obtained from publicly available datasets. The Southern Oscillation Index (SOI) and the Pacific Decadal Oscillation Index (PDO) were monthly region-wide indices (NOAA NCDC, 2017). Both indices were averaged for the swordfish spawning season, April – July. It is believed that swordfish spawn in Hawaiian waters and migrate there from regions where abundance is much higher, primarily the western Pacific (Sakagawa, 1989). The monthly el Niño Southern Oscillation (ENSO) index from region 3.4, the Oceanic Niño Index (ONI) was obtained from the NOAA Climate Prediction Center (NOAA NCEP CPC, 2017). Bigeye tuna vulnerability to longline gear has been shown to correlate with ENSO events as the overlap between their preferred habitat and the depth of the hooks set changes (Howell and Kobayashi, 2006).Lunar illumination data consisted of values between 0 and 1 that measured the proportion of the moon illuminated above Hawaii. It can be used as a proxy to indicate the lunar stage with 0 indicating a new moon and 1 indicating a full moon (US Naval Observatory, 2017). Swordfish CPUE has been shown to be highest during full moon events, potentially because swordfish are visual predators and more nocturnal illumination may make them more vulnerable to longline gear (Bigelow et al. 1999).

2.2 Vector-Autoregressive Spatio-Temporal (VAST) model

Relative abundance and density of swordfish were estimated using a multi-species VAST model (version 4.1.0) developed by James Thorson in Template Model Builder (TMB) version 1.7.13 via R version 3.3.4 (Kristensen et al., 2016; R Core Team, 2017; Thorson and Barnett, 2017; Thorson et al., 2017a). VAST estimates abundance using two models, one for the encounter rate and one for the positive catches. The configuration used in this analysis is a delta-lognormal generalized linear mixed model, which estimates the probability of encounter and positive catches from CPUE data. To increase computational speed, VAST estimates encounter probabilities and abundances for the spatial random effects fields at around 1,000 "knots". These knots were distributed equally throughout the data by applying a k-means clustering algorithm to the set of locations of all the samples (Thorson et al., 2017a). The density of the area around each

164   knot with a maximum radius of 150 km was then estimated from the delta-lognormal model (Fig.
165   1). The delta-lognormal GLMM (DL-GLMM) estimates relative density by breaking down the
166   catch information into two components: encounter probabilities p and positive catch rates r. The
167   formulation for the model is fully described in Thorson and Barnett (2017) and summarized here.
168   The spatio-temporal variation in encounter probability $p(s_i, c_i, t_i)$ uses a logit-linked linear
169   predictor in the form of:

$$\text{logit}[p(s_i, c_i, t_i)] = \gamma_p(c_i, t_i) + \varepsilon_p(s_i, c_i, t_i) + \delta_p(c_i, v_i) \tag{1}$$

170   where $\gamma_p(c_i, t_i)$ is the intercept for encounter probability for each taxon c and time t, $\varepsilon_p(s_i, c_i, t_i)$ is
171   the approximate spatio-temporal variation in encounter probability in logit-space, and $\delta_p(c_i, v_i)$ is
172   the random vessel effect v_i for the ith sample when catching taxon c_i. The expected catch rates for
173   each species encounter $r(s_i, c_i, t_i)$ is estimated using a log-linked linear predictor in the form of:

$$\log[r(s_i, c_i, t_i)] = \gamma_r(c_i, t_i) + \varepsilon_r(s_i, c_i, t_i) + \delta_r(c_i, v_i) \tag{2}$$

174   where $\gamma_r(c_i, t_i)$ is the intercept for expected catch rates for each taxon c and time t, $\varepsilon_r(s_i, c_i, t_i)$ is
175   the approximate spatio-temporal variation in expected catch rates in log-space, and $\delta_r(c_i, v_i)$ is the
176   random vessel effect v (Thorson and Barnett, 2017). The VAST model specifies a probability
177   distribution for the spatio-temporal variation (ε) using a three-dimensional Gaussian process
178   (equation 4 in Thorson and Barnett 2017). Due to the nature of the fishery, geometric anisotropy
179   was minimal and not included in the final model. The intercept and coefficient for spatial
180   temporal variation were estimated as annual fixed effect parameters and correlation between
181   species was estimated for both spatial and spatio-temporal components of the encounter rates and
182   positive catches models.
183   The multispecies model estimated the correlation between bigeye tuna and swordfish
184   using a spatial dynamic factor analysis that estimates a low-rank approximation to the spatial
185   distribution of multiple species simultaneously (Thorson et al., 2017a). When many species are
186   included, this provides the advantage of reducing the number of dimensions in the model.
187   However, with only two species, the primary advantage is to use the correlations between species
188   distribution to estimate relative abundance in time-periods when the shallow-set sector was
189   closed. This used a combination of factors less than or equal to the number of species to explain
190   the unobserved spatial (ω) and spatio-temporal (ε) variation for the two components of the delta
191   model (Thorson et al. 2015b, Eqns 5–7): the probability of a positive encounter and the positive
192   catch rates. For this analysis, a maximum of two factors was used to explain each of the four
193   spatial and spatial-temporal parameters. In addition, several catchability covariates were included
194   in both components of the DL-GLMM to help account for variance in the CPUE data, which was
195   not due to variance in relative abundance.
196   Several covariates were tested: quarter, month, time at which a set was started, hooks per
197   float, set type (tuna, billfish, or mixed), lunar illumination, and bait type. Of these, only lunar
198   illumination and set type resulted in converged models and were included in both components of
199   the final model. In addition, vessel, identified as the commercial fishing license number, was
200   included as a random effect that did not vary temporally. Parameters were estimated by
201   maximizing the marginal likelihood of the fixed effects: the intercept parameters for each
202   species, the covariation among species, and the included covariates while treating the spatio-
203   temporal variation, the vessel effect, and catchability variation as random effects using a Laplace
204   approximation (Thorson and Barnett, 2017). The final model was checked for convergence, and
205   diagnostics were run to evaluate model fit. VAST provides a variety of outputs including an

206 annual index of abundance, a map of relative density, QQ plots, center of gravity estimates,
207 effective area estimates, residual plots, and plots of the density CVs.
208   Within the VAST framework, variables are included as either a catchability variable
209 changes the proportion of the fish that are caught or a density variable that affects the density of
210 the fish in an area. All of the variables included in the VAST model are catchability variables,
211 however, it can be difficult to identify if some environmental variables affect catchability,
212 density, or both. Therefore, we did a post-hoc correlation exploration of the environmental
213 variables ONI, SOI, and PDO to see if they were correlated to swordfish distribution. We ran a
214 simple linear regression on the Easting and Northing components of the estimated center of
215 gravity and estimated effective area for swordfish for each of the three environmental variables
216 and calculated the correlation coefficients for each.

3. Results

218 The distribution of annual swordfish density showed high densities in the northernmost latitudes
219 of the Hawaii-based longline fishing grounds (Fig. 1), and much lower densities around the
220 Hawaiian Islands (Fig. 2). Abundance appeared to be highest at the start of the swordfish fishery
221 (1995–2000) and decreased after 2000 (Fig. 3). Since 2005, the relative abundance trend appears
222 to be relatively stable. Model diagnostics suggested the model converged, with good fits and
223 some minor patterning in the residuals (Supplemental Fig. S1–S4). Standardized residuals for
224 abundance around each knot were also relatively small, the majority between 2 and -2, and no
225 apparent trend (Supplemental Fig. S5). Relative abundance appeared to be well estimated, with
226 small CVs around most of the knots except for some locations to the far east and south, which
227 marked the edges of the main fishing grounds and had the fewest data points. Also, CVs around
228 estimates of abundance increased between 2001 and 2004, which coincided with the shutdown of
229 the shallow-set fishery (Supplemental Fig. S6). Estimated coefficients for lunar illumination and
230 set type were significant and the confidence intervals (C.I.) did not cross zero for both the
231 encounter probability (mean 0.12, C.I. 0.10 – 0.14 and mean 2.52, C.I. 2.48-2.56) and the
232 positive catch rates (mean 0.064, C.I. 0.070-0.057 and mean 1.49, C.I. 1.47-1.50, respectively).
233   The spatial dynamic factor analysis used two factors to explain the unobserved spatial
234 and spatio-temporal variations between swordfish and bigeye tuna abundance. Correlation
235 between these two species was strongly positive for both the encounter probability and positive
236 catch rate spatial variability, and not correlated for the spatio-temporal variability (Fig. 4).
237   The center of gravity and effective area covered by swordfish in the Hawaii-based
238 longline fishing grounds was highly variable and without consistent trend in the area or in the
239 east-west component (Fig. 5). Comparison of these time series with some major climatological
240 indices, however, suggested that there was a correlation between the center of gravity of
241 swordfish abundance and the average SOI during the swordfish spawning season, April–July
242 (Fig. 6). There did not appear to be any correlation between the center of gravity and the PDO or
243 the ONI (Supplemental Figs S7–S10). The SOI was more strongly correlated with the latitudinal
244 location of the swordfish center of gravity ($\rho = 0.42$) than the longitudinal location of the
245 swordfish center of gravity ($\rho = 0.35$, Fig. 7). A simple linear regression run on the center of
246 gravity time series with SOI as an explanatory variable was statistically significant for the
247 longitudinal component ($R^2 = 0.17$, p = 0.05) but not for the latitudinal component ($R^2 = 0.12$, p =
248 0.11). Generally, swordfish were found further to the east and north during periods of positive
249 SOI, which is associated with cooler waters and La Niña conditions and further to the east and
250 south during periods of negative SOI which is associated with warmer waters and El Niño
251 conditions (NOAA NCDC, 2017).

4. Discussion

We attempted to produce estimates of swordfish abundance from the Hawaii-based longline fishery using the spatial dynamic factors estimated between swordfish and bigeye tuna catches to account for periods when the shallow-set sector was closed or fishermen recorded sets as mixed targeting (which occurred prior to the closure; (He et al., 1997). This had the advantage of using the complete data set and estimating abundance for years when the fishery was entirely or partially closed. While there are still some clear trends in the data which correlate to before and after the fishery closure and regulation changes in 2000, the density of swordfish within the Hawaii-based longline fishing grounds appears to be consistent with previous findings and appears to also be reliable (Bigelow et al., 1999; He et al., 1997; Polovina et al., 2001; Sculley et al., 2018b; Seki et al., 2002).

In the Hawaii-based longline fishery, the largest catches occur along the Sub-Tropical Convergence Zone (STCZ) located around 25–35°N latitude (Bigelow et al., 1999; Seki et al., 2002), which was the same area of high density described in the current study. This region also shifts seasonally and in response to the ENSO cycle. The STCZ shifts further to the south during el Niño events and northward during la Niña events (Howell et al., 2012; Polovina et al., 2001). This corresponds to the shift in the center of gravity of swordfish density and suggests that swordfish may be following the movement of this convergence zone. Rather than responding to the temperatures directly, it is likely that they are following their prey, as this is a highly productive region and a known area where swordfish feed (Polovina et al., 2001).

Incorporating catchability covariates in the model was a challenge. Many of the operational variables, such as time the set began and the number of hooks per float, which were correlated with swordfish CPUE and have been used in more traditional delta-lognormal models for CPUE standardization, could not be included in this analysis because the model failed to converge. As a result, it was clear that there are still some catchability covariates, which were unaccounted for based upon the change in annual relative abundance for swordfish before and after the 2000 closure. Another challenge was how to incorporate environmental covariates. In traditional standardization methods, the estimate of relative abundance is extracted from the annual effect of the standardization model (Maunder and Punt, 2004), which can include explanatory variables which predict catchability and which predict abundance. VAST uses explanatory variables that predict abundance to provide density estimates but does not include catchability variables (Thorson, 2018). Therefore, in the model development users must specify if which covariate a component predicts. Environmental variables, such as mixed layer depth, sea surface temperature, and climatological indices, which were correlated with swordfish CPUE, may influence both catchability and abundance. This means that it can be challenging to know how to include these types of variables in the VAST modeling framework, and we may be losing an important explanatory variable for the trends and patterns we observed.

VAST was originally developed to analyze fishery-independent data in the North Pacific Ocean and works very well with data which are collected regularly across the species' distribution (Cao et al., 2017; Thorson et al., 2015a; Thorson et al., 2015b; Thorson et al., 2016; Thorson et al., 2017b). Work is also currently being conducted to use VAST for other highly migratory species, such as the tropical tunas and pelagic sharks. However, these data cover the majority of the distribution of the species (Kai, 2019; Xu et al., 2019). The Hawaii-based longline fishery targets a small proportion of the distribution of North Pacific swordfish and does not encompass the primary fishing grounds in the western Pacific. It is highly likely that swordfish density changes throughout the year. Therefore, annual estimates of swordfish density

298 may not be as useful as examining seasonal densities. Estimating seasonal densities may be
299 limited by computing power. The Hawaii-based longline set-by-set data are not large compared
300 to other longline fleets in the Pacific Ocean. However, the number of knots used compared to the
301 area was limited by memory limitations, and the model could take hours to days to run. A
302 quarterly time step would increase memory requirements and may only be possible on a
303 supercomputer or other high-performance computing system. Aggregating the data spatially
304 would reduce some of this need, but would also reduce the performance of the spatial models
305 (Thorson et al., 2017a).
306   North Pacific swordfish assessments have shown periodic strong year classes, which
307 were correlated with the spawning season SOI (Sculley et al., 2018a). It was unsurprising to find
308 that the SOI correlated with swordfish distribution around the Hawaiian spawning grounds as
309 well. It is possible that changes in swordfish distribution around Hawaii are driven by these
310 strong pulses of recruitment or that the changes in recruitment strength are due to changes in
311 swordfish distribution around Hawaii. Brodziak et al. (2010) found a strong negative correlation
312 between swordfish recruits per spawner anomalies and the spawning season SOI (ρ = -0.55, p
313 <0.001). An update of that analysis using the most recent stock assessment (ISC, 2018) showed a
314 similar negative correlation between the SOI during the spawning season and swordfish recruits
315 per spawning biomass during 1975–2016 (ρ = -0.43, p <0.005, Fig.8). Young-of-the-year
316 swordfish appear in the Hawaii-based fishery in September–October of each year, based upon
317 the pulse of 50–80cm fish caught (Sculley et al., 2017). The majority of the young-of-the-year
318 fish are caught in the tuna-targeting deep-set fishery and appear to be spatially separate from the
319 adults. While the adults are caught primarily around the STCZ, juvenile swordfish are caught
320 south of the Hawaiian Islands (Sculley et al., 2017). It is possible the swordfish are moving in
321 response to oceanographic variables, such as sea surface temperature and the location of the
322 subtropical frontal zone during the spawning season, which could influence the success of
323 recruitment, noting that swordfish larvae are most commonly observed in warmer waters above
324 24°C (Nakamura, 1985). This may result in some swordfish spawning in areas with less-than-
325 ideal water temperatures for successful recruitment or in areas with too little prey for the larvae.
326 Alternatively, the swordfish could be spawning in areas with stronger currents, which may move
327 swordfish recruits out of the Hawaii-based longline fishing grounds and, therefore, would not
328 appear in the fishery later that year.
329   Highly mobile species, such as swordfish, can respond quickly to annual variation in
330 temperature. Determining how species respond to these changes can provide insights into how
331 they may respond to future climate change (Morley et al., 2017) and how those changes may
332 affect the viability of the Hawaii-based longline fishery. Swordfish center of gravity was located
333 more southerly and westerly during periods of warmer surface temperatures (negative SOI). If
334 future sustained oceanic conditions are more similar to those observed during a negative SOI, we
335 may expect the swordfish in the Hawaii-based fishing grounds to shift their biomass in a similar
336 pattern. Additional work incorporating sea surface temperature, mixed layer depth, dissolved
337 oxygen concentrations, or food quality metrics, such as phytoplankton size, would provide
338 additional insight on how swordfish may respond to climate change. Ultimately, a better
339 understanding on how highly migratory species respond to climate change is an important
340 research question and could have significant economic and cultural impacts on the Hawaii-based
341 commercial longline fishery.

References

Abecassis, M.,Dewar, H.,Hawn, D.,Polovina, J., 2012. Modeling swordfish daytime vertical habitat in the North Pacific Ocean from pop-up archival tags. Mar. Ecol. Prog. Ser. 452, 219-236. 10.3354/meps09583.

Bigelow, K.A.,Boggs, C.H.,He, X., 1999. Environmental effects on swordfish and blue shark catch rates in the US North Pacific longline fishery. Fish. Oceanogr. 8, 178-198. DOI 10.1046/j.1365-2419.1999.00105.x.

Boggs, C.H.,Ito, R.Y., 1993. Hawaii's pelagic Fisheries. Mar. Fish. Rev. 55, 69-82.

Brodziak, J.,Courtney, D.,Piner, K.,Lee, H.H.,DiNardo, G., 2010. Modeling recruitment responses of striped marlin (Tetrapturus audax) and swordfish (Xiphias gladius) to environmental variability in the North Pacific. PICES International Symposium: Climate Change Effects on Fish and Fisheries, April 25-29, 2010. Presentation.

Campbell, R.A., 2004. CPUE standardisation and the construction of indices of stock abundance in a spatially varying fishery using general linear models. Fish. Res. 70, 209-227. https://doi.org/10.1016/j.fishres.2004.08.026.

Cao, J.,Thorson, J.T.,Richards, R.A.,Chen, Y., 2017. Spatiotemporal index standardization improves the stock assessment of northern shrimp in the Gulf of Maine. Can. J. Fish. Aquat. Sci. 74, 1781-1793. 10.1139/cjfas-2016-0137.

Chang, Y.J.,Sun, C.L.,Chen, Y.,Yeh, S.Z.,DiNardo, G.,Su, N.J., 2013. Modelling the impacts of environmental variation on the habitat suitability of swordfish, Xiphias gladius, in the equatorial Atlantic Ocean. ICES J. Mar. Sci. 70, 1000-1012. 10.1093/icesjms/fss190.

Demartini, E.,Uchiyama, J.H.,Williams, H.A., 2000. Sexual maturity, sex ratio, and size composition of swordfish, Xiphias gladius, caught by the Hawaii-based pelagic longline fishery. Fish. Bull. 98, 489-506.

DeMartini, E.E.,Uchiyama, J.H.,Humphreys, R.L.,Sampaga, J.D.,Williams, H.A., 2007. Age and growth of swordfish (*Xiphias gladius*) caught by the Hawaii-based pelagic longline fishery. Fish. Bull. 105, 356-367.

Dewar, H.,Prince, E.D.,Musyl, M.K.,Brill, R.W.,Sepulveda, C.,Luo, J.G.,Foley, D.,Orbesen, E.S.,Domeier, M.L.,Nasby-Lucas, N.,Snodgrass, D.,Laurs, R.M.,Hoolihan, J.P.,Block, B.A.,McNaughton, L.M., 2011. Movements and behaviors of swordfish in the Atlantic and Pacific Oceans examined using pop-up satellite archival tags. Fish. Oceanogr. 20, 219-241. 10.1111/j.1365-2419.2011.00581.x.

Gilman, E.,Kobayashi, D.,Swenarton, T.,Brothers, N.,Dalzell, P.,Kinan-Kelly, I., 2007. Reducing sea turtle interactions in the Hawaii-based longline swordfish fishery. Biol. Conserv. 139, 19-28. 10.1016/j.biocon.2007.06.002.

He, X.,Bigelow, K.A.,Boggs, C.H., 1997. Cluster analysis of longline sets and fishing strategies within the Hawaii-based fishery. Fish. Res. 31, 147-158. Doi 10.1016/S0165-7836(96)00564-4.

Howell, E.A.,Kobayashi, D.R., 2006. El Niño effects in the Palmyra Atoll region: oceanographic changes and bigeye tuna (Thunnus obesus) catch rate variability. Fish. Oceanogr. 15, 477-489. 10.1111/j.1365-2419.2005.00397.x.

387 Howell, E.A.,Kobayashi, D.R.,Parker, D.M.,Balazs, G.H.,Polovina a, J.J., 2008. TurtleWatch: a tool to aid in
388   the bycatch reduction of loggerhead turtles Caretta caretta in the Hawaii-based pelagic longline
389   fishery. Endangered Species Research. 5, 267-278.
390 Howell, E.A.,Bograd, S.J.,Morishige, C.,Seki, M.P.,Polovina, J.J., 2012. On North Pacific circulation and
391   associated marine debris concentration. Mar. Pollut. Bull. 65, 16-22.
392   https://doi.org/10.1016/j.marpolbul.2011.04.034.
393 Ichinokawa, M.,Brodziak, J., 2010. Using adaptive area stratification to standardize catch rates with
394   application to North Pacific swordfish (Xiphias gladius). Fish. Res. 106, 249-260.
395   10.1016/j.fishres.2010.08.001.
396 ISC, 2018. Stock Assessment for Swordfish (Xiphias gladius) in the Western and Central North Pacific
397   Ocean through 2016. Annex 16. ISC/18/ANNEX/16, 84.
398   http://isc.fra.go.jp/pdf/ISC18/ISC_18_ANNEX_16_Stock_Assessment_of_WCNPO_Swordfish_thr
399   ough_2016_FINAL.pdf.
400 Ito, R.,Childers, J., 2018. U.S. swordfish fisheries in the North Pacific Ocean. ISC/18/BILLWG/01.
401   http://isc.fra.go.jp/reports/bill/bill_2018_1.html.
402 Kai, M., 2019. Spatio-temporal changes in catch rates of pelagic sharks caught by Japanese research and
403   training vessels in the western and central North Pacific. Fish. Res. 216, 177-195.
404   https://doi.org/10.1016/j.fishres.2019.02.015.
405 Kristensen, K.,Nielsen, A.,Berg, C.W.,Skaug, H.,Bell, B.M., 2016. TMB: Automatic Differentiation and
406   Laplace Approximation. Journal of Statistical Software. 70, 1-21. doi:10.18637/jss.v070.i05.
407 Lu, C.P.,Smith, B.L.,Hinton, M.G.,Bremer, J.R.A., 2016. Bayesian analyses of Pacific swordfish (Xiphias
408   gladius L.) genetic differentiation using multilocus single nucleotide polymorphism (SNP) data. J.
409   Exp. Mar. Biol. Ecol. 482, 1-17. 10.1016/j.jembe.2016.03.010.
410 Maunder, M.N.,Punt, A.E., 2004. Standardizing catch and effort data: a review of recent approaches.
411   Fish. Res. 70, 141-159. 10.1016/j.fishres.2004.08.002.
412 Morley, J.W.,Batt, R.D.,Pinsky, M.L., 2017. Marine assemblages respond rapidly to winter climate
413   variability. Glob Chang Biol. 23, 2590-2601. 10.1111/gcb.13578.
414 Nakamura, I., 1985. Billfishes of the world. FAO Fish. Synop. 125.
415 [dataset] NMFS, 2017. Hawaii longline fishery logbook statistics -non-confidential summary tables. .
416   http://www.pifsc.noaa.gov/fmb/reports.php.
417 [dataset] NOAA NCDC, 2017. Spatially and temporally large-scale anomalies that influence the variability
418   of the atmospheric circulation. . https://www.ncdc.noaa.gov/teleconnections/.
419 [dataset] NOAA NCEP CPC, 2017. Historical El Nino / La Nina episodes (1950-present).
420   http://origin.cpc.ncep.noaa.gov/products/analysis_monitoring/ensostuff/ONI_v5.php.
421 Pacheco, J.C.,Kerstetter, D.W.,Hazin, F.H.,Hazin, H.,Segundo, R.S.S.L.,Graves, J.E.,Carvalho, F.,Travassos,
422   P.E., 2011. A comparison of circle hook and J hook performance in a western equatorial Atlantic
423   Ocean pelagic longline fishery. Fish. Res. 107, 39-45.
424   https://doi.org/10.1016/j.fishres.2010.10.003.
425 Pacific Islands Regional Office, 2017. Hawaii Longline Observer Program Observer Field Manual. Version
426   LM.17.02. . in: National Oceanic and Atmospheric Administration P.I.R., ed. Honolulu, Hawaiʻi.
427 Pacific Islands Regional Office, 2018. Regulation Summary Hawaii Pelagic Longline Fishing. in: Commerce
428   N.O.a.A.D.o., ed: National Marine Fisheries Service.
429 Pennino, M.G.,Conesa, D.,López-Quílez, A.,Muñoz, F.,Fernández, A.,Bellido, J.M., 2016. Fishery-
430   dependent and -independent data lead to consistent estimations of essential habitats. ICES J.
431   Mar. Sci. 73, 2302-2310. 10.1093/icesjms/fsw062.
432 Polovina, J.J.,Howell, E.,Kobayashi, D.R.,Seki, M.P., 2001. The transition zone chlorophyll front, a
433   dynamic global feature defining migration and forage habitat for marine resources. Prog.
434   Oceanogr. 49, 469-483. https://doi.org/10.1016/S0079-6611(01)00036-2.

435 Prince, E.D.,Ortiz, M.,Venizelos, A., 2002. A comparison of circle hook and "J" hook performance in
436   recreational catch-and-release fisheries in billfish. in: Lucy J.A., Studholme A.L., eds. Catch and
437   Release in Marine Recreational Fisheries. American Fisheries Society, Bethesda, Maryland,
438 Prince, E.D.,Goodyear, C.P., 2006. Hypoxia-based habitat compression of tropical pelagic fishes. Fish.
439   Oceanogr. 15, 451-464. 10.1111/j.1365-2419.2005.00393.x.
440 R Core Team, 2017. R: A language and environment for statistical computing. Vienna, Austria.: R
441   Foundation for Statistical Computing.
442 Sakagawa, G.T., 1989. Trends in fisheries for swordfish in the Pacific Ocean. In: Planning the Future of
443   Billfishes: Research and Management in the 90s and Beyond. in: Stroud R.H., ed. Proceedings of
444   the Second International Billfish Symposium, Kailua-Kona, Hawaii, 1–5 August 1988, Part 1:
445   Fishery and Stock Synopses, Data Needs and Management. National Coalition for Marine
446   Conservation, Savannah, GA, 61-79.
447 Sculley, M.,Brodziak, J.,Yau, A.,Kapur, M., 2017. An Exploratory Analysis of Trends in Swordfish (Xiphias
448   gladius) Length Composition Data from the Hawaiian Longline Fishery. Pacific Islands Fisheries
449   Science Center, PIFSC Working Paper. WP-17-002, 48. https://doi.org/10.7289/V5/WP-PIFSC-17-
450   002.
451 Sculley, M.,Ijima, H.,Chang, Y.-J., 2018a. A base-case model in stock synthesis 3.30 for the 2018 North
452   Pacific swordfish (Xiphias gladius) stock assessment. Pacific Islands Fisheries Science Center,
453   PIFSC Working Paper. WP-18-005, 39. https://doi.org/10.7289/V5/WP-PIFSC-18-003.
454 Sculley, M.,Yau, A.,Kapur, M., 2018b. Standardization of the Swordfish Xiphias gladius Catch per Unit
455   Effort Data Caught by the Hawaii-based Longline Fishery from 1994-2016 Using Generalized
456   Linear Models. Pacific Islands Fisheries Science Center, PIFSC Working Paper. WP-18-001, 50.
457   https://doi.org/10.7289/V5/WP-PIFSC-18-001.
458 Seki, M.P.,Polovina, J.J.,Kobayashi, D.R.,Bidigare, R.R.,Mitchum, G.T., 2002. An oceanographic
459   characterization of swordfish (Xiphias gladius) longline fishing grounds in the springtime
460   subtropical North Pacific. Fish. Oceanogr. 11, 251-266. doi:10.1046/j.1365-2419.2002.00207.x.
461 Thorson, J.T.,Ianelli, J.N.,Munch, S.B.,Ono, K.,Spencer, P.D., 2015a. Spatial delay-difference models for
462   estimating spatiotemporal variation in juvenile production and population abundance. Can. J.
463   Fish. Aquat. Sci. 72, 1897-1915. 10.1139/cjfas-2014-0543.
464 Thorson, J.T.,Scheuerell, M.D.,Shelton, A.O.,See, K.E.,Skaug, H.J.,Kristensen, K.,Warton, D., 2015b.
465   Spatial factor analysis: a new tool for estimating joint species distributions and correlations in
466   species range. Methods Ecol. Evol. 6, 627-637. 10.1111/2041-210x.12359.
467 Thorson, J.T.,Ianelli, J.N.,Larsen, E.A.,Ries, L.,Scheuerell, M.D.,Szuwalski, C.,Zipkin, E.F., 2016. Joint
468   dynamic species distribution models: a tool for community ordination and spatio-temporal
469   monitoring. Global Ecol. Biogeogr. 25, 1144-1158. 10.1111/geb.12464.
470 Thorson, J.T.,Barnett, L.A.K., 2017. Comparing estimates of abundance trends and distribution shifts
471   using single- and multispecies models of fishes and biogenic habitat. ICES J. Mar. Sci. 74, 1311-
472   1321. 10.1093/icesjms/fsw193.
473 Thorson, J.T.,Fonner, R.,Haltuch, M.A.,Ono, K.,Winker, H., 2017a. Accounting for spatiotemporal
474   variation and fisher targeting when estimating abundance from multispecies fishery data. Can. J.
475   Fish. Aquat. Sci. 74, 1794-1807. 10.1139/cjfas-2015-0598.
476 Thorson, J.T.,Ianelli, J.N.,Kotwicki, S., 2017b. The relative influence of temperature and size-structure on
477   fish distribution shifts: A case-study on Walleye pollock in the Bering Sea. Fish Fish. 18, 1073-
478   1084. 10.1111/faf.12225.
479 Thorson, J.T., 2018. VAST User Manual. https://github.com/James-Thorson-
480   NOAA/VAST/tree/master/manual.
481 US Naval Observatory, 2017. Fraction of the Moon Illuminated at Midnight Hawaiian-Aleutian Standard
482   Time. in: Observatory U.N., ed.

483   Walsh, W., 2000. Comparisons of fish catches reported by fishery observers and in logbooks of Hawaii-
484   based commercial longline vessels. Southwest Fisheries Science Center Honolulu Laboratory,
485   National Marine Fisheries Service, NOAA. Honolulu, HI. Southwest Fisheries Science Center
486   Administrative Report H-00-07, 45. https://drive.google.com/file/d/1O_GRLxzvYhTuN7DcEC8V-
487   bPTNYs21NwE/view.
488   Walters, C., 2003. Folly and fantasy in the analysis of spatial catch rate data. Can. J. Fish. Aquat. Sci. 60,
489   1433-1436. 10.1139/f03-152.
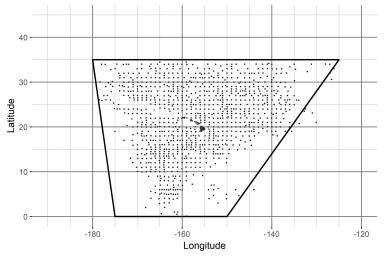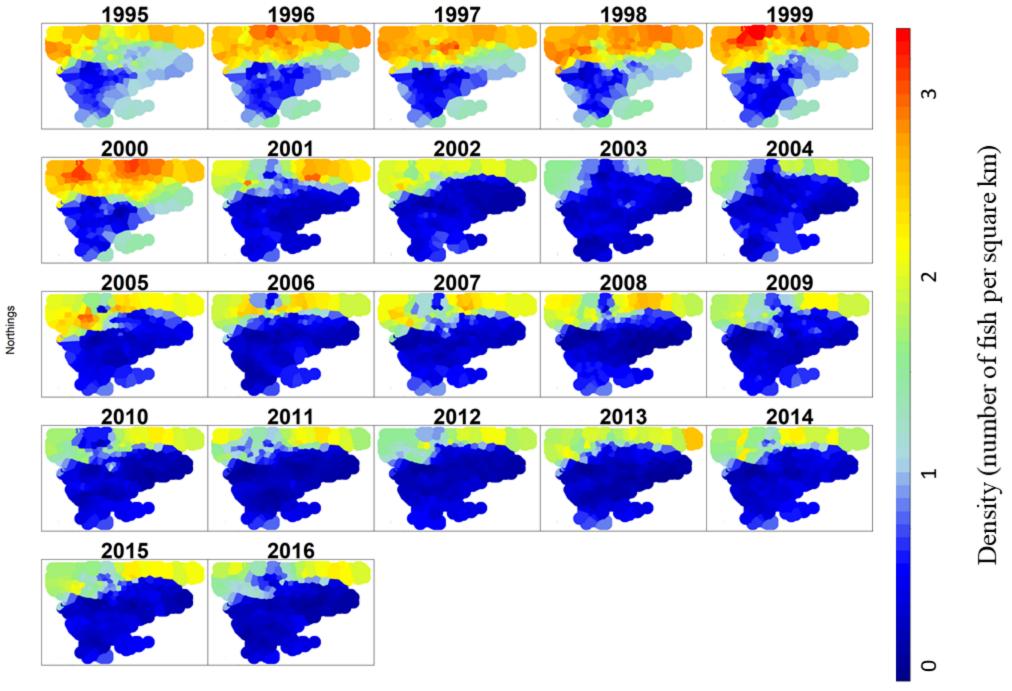490   Wilberg, M.J.,Thorson, J.T.,Linton, B.C.,Berkson, J., 2009. Incorporating Time-Varying Catchability into
491   Population Dynamic Stock Assessment Models. Rev. Fish. Sci. 18, 7-24.
492   10.1080/10641260903294647.
493   Xu, H.,Lennert-Cody, C.E.,Maunder, M.N.,Minte-Vera, C.V., 2019. Spatiotemporal dynamics of the
494   dolphin-associated purse-seine fishery for yellowfin tuna (Thunnus albacares) in the eastern
495   Pacific Ocean. Fish. Res. 213, 121-131. https://doi.org/10.1016/j.fishres.2019.01.013.
496   Ye, Y.,Mohammed, M.A., 1999. An analysis of variation in catchability of green tiger prawn, Penaeus
497   semisulcatus, in waters off Kuwait. Fish. Bull. 97, 702-712.

498
499

500 *Figure 1*. Distribution of knots used to estimate the density of swordfish (points) and the
501 approximate extent of the Hawaii-based fishery (box).
502 *Figure 2*. Density of swordfish abundance by year in number of fish per square km.
503 *Figure 3*. Estimated annual relative abundance of swordfish. Grey shading indicates the 95%
504 confidence interval. The fishery targetting swordfish fishery was closed from 2000-2004.
505 *Figure 4.* Correlation matrix for swordfish and bigeye tuna for the spatial (right) and spatio-
506 temporal (left) variance for encounter probability (component 1, top) and positive catch rate
507 (component 2, bottom). Darker colors indicate a higher correlation.
508 *Figure 5*. Center of gravity for the east-west component (top left) and north-south component
509 (top right) and effective area (bottom left) estimates for swordfish. Grey shading indicates 95%
510 confidence intervals.
511 *Figure 6*. Normalized center of gravity (Easting, top left, Northing, top right) and effective area
512 (bottom left) with normalized average SOI in April-July (red=positive SOI, blue=negative SOI).
513 *Figure 7*. Center of gravity (Easting, top, Northing, bottom) versus SOI with linear regression
514 (blue line) and 95% confidence intervals (grey shading). The correlation between SOI and each
515 direction are on each plot.
516 *Figure 8.* Recruits per spawning biomass versus average SOI (April-July). The blue line
517 indicates fit to a linear regression with 95% confidence interval (dashed lines), Pearson
518 correlation coefficient of $\rho=-0.43$ and p-value of $P<0.001$.
519
520

Correlation = 0.36

Correlation = 0.34

Recruits per spawning biomass (kg) versus Southern Oscillation Index (April-July average)